


An analytical solution of the inverse problem of capillary imbibition

Cite as: Phys. Fluids **32**, 041704 (2020); <https://doi.org/10.1063/5.0008081>

Submitted: 18 March 2020 . Accepted: 06 April 2020 . Published Online: 23 April 2020

Sufia Khatoon, Jyoti Phirani, and Supreet Singh Bahga 



View Online



Export Citation



CrossMark



An analytical solution of the inverse problem of capillary imbibition

Cite as: Phys. Fluids 32, 041704 (2020); doi: 10.1063/5.0008081

Submitted: 18 March 2020 • Accepted: 6 April 2020 •

Published Online: 23 April 2020



Sufia Khatoon,¹ Jyoti Phirani,² and Supreet Singh Bahga^{1,a)}

AFFILIATIONS

¹Department of Mechanical Engineering, Indian Institute of Technology, Delhi 110016, India

²Department of Chemical Engineering, Indian Institute of Technology, Delhi 110016, India

^{a)}Author to whom correspondence should be addressed: bahga@mech.iitd.ac.in

ABSTRACT

The inverse problem of capillary imbibition involves determination of the capillary geometry from the measurements of the time-varying meniscus position. This inverse problem is known to have multiple solutions, and to ensure a unique solution, measurements of imbibition kinematics in both directions of the capillary are required. We here present a closed-form analytical solution of the inverse problem of determining the axially varying radius of a capillary from experimental data of the meniscus position as a function of time. We demonstrate the applicability of the method for solving the inverse capillary imbibition problem for two cases, wherein the data for imbibition kinematics are obtained (i) using numerical simulations and (ii) from published experimental work. In both cases, the axially varying capillary radius predicted by the analytical solution agrees with the true capillary radius. In contrast to the previously proposed iterative methods for solving the inverse capillary imbibition problem, the analytical method presented here yields a direct solution. This analytical solution of the inverse capillary imbibition problem can be helpful in determining the internal geometry of micro- and nano-porous structures in a non-destructive manner and design of autonomous capillary pumps for microfluidic applications.

Published under license by AIP Publishing. <https://doi.org/10.1063/5.0008081>

The penetration of a liquid into a capillary due to the wetting of the liquid on the walls, known as capillary imbibition, is of relevance to diverse fields including enhanced oil recovery,¹ groundwater pollution,² flow through porous media,^{3,4} tissue drug delivery,⁵ and microfluidic systems.⁶ The forward problem of determining the meniscus position $\ell(t)$ vs time t has been studied extensively in the past for various geometric and flow configurations.^{7–12} However, the inverse problem of determining the capillary geometry from measured ℓ vs t data¹³ has received comparatively less attention. The inverse problem of capillary imbibition is of significant importance as it can be used to determine the geometry of those capillaries, such as nano-pores,¹⁴ which otherwise cannot be directly visualized. The solution of the inverse problem can also be used to design autonomous microfluidic capillary pumps with desired flow characteristics.^{14,15}

In this paper, we consider the inverse problem of determining the axially varying radius of an axisymmetric, non-uniform cross section capillary, illustrated in Fig. 1, from the measured imbibition kinematics. As shown in Fig. 1, the liquid filled in either the

left or the right reservoir, maintained at atmospheric pressure, wets the capillary wall, and penetrates into the horizontally oriented capillary. The left and the right ends of the capillary are at $x = 0$ and $x = L$, respectively. The imbibition process is characterized by the time-varying meniscus position $x = \ell(t)$. In the regime, where viscous dissipation dominates flow inertia, the meniscus speed $u(\ell) = d\ell/dt$ is governed by¹³

$$\frac{d\ell}{dt} = \frac{\gamma \cos(\theta)}{4\mu r(\ell)^3 \int_0^\ell r(x)^{-4} dx}. \quad (1)$$

Here, x is the axial coordinate along the capillary, $r(x)$ is the axially varying capillary radius, μ is the dynamic viscosity of the liquid, γ is the air-liquid surface tension, and θ is the contact angle made by the liquid with the capillary wall. The above equation is based on the assumption of slow axial variations in the capillary radius.¹⁰ The contact angle θ in this equation can be taken as the equilibrium contact angle only for quasi-static motion of the meniscus on ideal surfaces. However, because the meniscus is moving and for

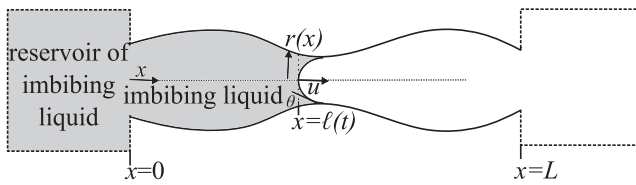


FIG. 1. Schematic illustrating imbibition in an axisymmetric capillary with an axially varying cross section. During forward imbibition, the liquid meniscus moves from $x = 0$ to L , whereas for imbibition in the reverse direction, the meniscus moves from $x = L$ to 0 . The meniscus position during forward and reverse imbibition is denoted by $x = \ell(t)$. The meniscus moves with a mean flow speed given by u and makes a contact angle θ with the capillary wall.

systems with significant contact angle hysteresis, θ should be replaced with the receding contact angle.¹⁰ Equation (1) can be easily solved to obtain a unique solution for the meniscus position $\ell(t)$ if the capillary radius $r(x)$ is known.^{9,10} However, the inverse problem of determining the radius $r(x)$ of a non-uniform capillary, from experimentally measured imbibition kinematics (ℓ vs t) or meniscus speed $u(\ell) = d\ell/dt$, is ill-posed. Elizalde *et al.*¹³ showed that an infinite family of curves $r(x)$ can produce the same meniscus velocity $u(\ell)$. They also showed that a unique solution for $r(x)$ can be ensured if the experimental data for capillary imbibition in both directions, that is, from $x = 0$ to L and from $x = L$ to 0 , are used to solve the inverse problem.

The previous works on the solution of the inverse capillary imbibition problem^{13,14} are based on an iterative, numerical procedure to reproduce experimentally observed ℓ vs t curves for imbibition in both directions. In this method, first a family of curves $r(x)$ is obtained that reproduces the kinematics of imbibition in one direction, using Eq. (1). Among these $r(x)$ curves, that particular curve is chosen which is able to predict the experimentally measured data for imbibition in the opposite direction, using Eq. (1). In contrast to this iterative approach, we here present a closed-form analytical solution for the inverse problem of determining the capillary radius $r(x)$ that reproduces the measured ℓ vs t curves for imbibition in forward and reverse directions. Our analytical method gives a direct solution to the inverse problem of capillary imbibition, which is a significant improvement over the iterative methods proposed earlier.

This paper is structured as follows: First, we derive a closed-form analytical solution to the inverse problem of capillary imbibition. Thereafter, we present validation of the analytical solution by considering two inverse problems, wherein the data for imbibition kinematics are obtained from numerical simulations and experiments. This is followed by concluding remarks on significance and applications of this work.

Our method is based on simultaneous consideration of the capillary imbibition process in forward and reverse directions. From Eq. (1), the meniscus speeds during imbibition in forward and reverse directions, respectively, denoted by subscripts f and r , are given by

$$u_f(\ell) = \frac{d\ell}{dt} = \frac{\gamma \cos(\theta)}{4\mu r(\ell)^3 \int_0^\ell r(x)^{-4} dx}, \quad (2)$$

$$u_r(\ell) = -\frac{d\ell}{dt} = \frac{\gamma \cos(\theta)}{4\mu r(\ell)^3 \int_\ell^L r(x)^{-4} dx}. \quad (3)$$

Here, the negative sign in $u_r(\ell) = -d\ell/dt$ denotes that $\ell(t)$ (measured from $x = 0$) decreases with time during imbibition from $x = L$ to 0 . Equations (2) and (3) can be combined as follows:

$$I = \int_0^L r(x)^{-4} dx = \int_0^\ell r(x)^{-4} dx + \int_\ell^L r(x)^{-4} dx, \quad (4)$$

$$= \frac{\gamma \cos(\theta)}{4\mu r(\ell)^3} \left[\frac{1}{u_f(\ell)} + \frac{1}{u_r(\ell)} \right]. \quad (5)$$

This equation can be written in a compact form by defining $\alpha = \gamma \cos(\theta)/\mu$ and $f(\ell) = (u_f(\ell)^{-1} + u_r(\ell)^{-1})/4$ to get

$$I = \int_0^L r(x)^{-4} dx = \frac{\alpha}{r(\ell)^3} f(\ell). \quad (6)$$

Note that the integral I is related to the hydraulic resistance of the completely filled capillary. In addition, I remains constant over the imbibition process. The quantity $f(\ell)$ is obtained from experimental measurements of imbibition speeds in both directions. From Eq. (6), the radius of the capillary $r(\ell)$ can be obtained as

$$r(\ell) = \left(\frac{\alpha f(\ell)}{I} \right)^{1/3}. \quad (7)$$

The only unknown in this equation is I , which can be obtained by substituting the above relation for radius in the definition of I , given by Eq. (4), to get

$$I = \int_0^L r(x)^{-4} dx = \int_0^L \left[\frac{\alpha f(x)}{I} \right]^{-4/3} dx \\ = \left(\frac{I}{\alpha} \right)^{4/3} \int_0^L f(x)^{-4/3} dx. \quad (8)$$

Therefore, I is given by

$$I = \frac{\alpha^4}{\left(\int_0^L f(x)^{-4/3} dx \right)^3}. \quad (9)$$

Finally, substituting the expression for I given by Eq. (9) in Eq. (7), we arrive at a closed-form relation for the axially varying radius $r(x)$ of the capillary,

$$r(x) = \frac{f(x)^{1/3}}{\alpha} \int_0^L f(\eta)^{-4/3} d\eta. \quad (10)$$

Knowing the measured values of $f(x) = (u_f(x)^{-1} + u_r(x)^{-1})/4$ at various axial locations x along the capillary, the above equation can be used to directly determine the radius curve $r(x)$. We note that random uncertainties in experimental measurements can result in a random noise in the measured values of $f(x)$. Therefore, a smoothing filter can be applied on $f(x)$ prior to estimation of $r(x)$, using Eq. (10).

To validate our method, we considered two inverse problems, wherein the data for imbibition kinematics are obtained (i) using numerical simulations and (ii) from experiment data of Elizalde

*et al.*¹³ For the first problem, we assumed a capillary of length $L = 30$ mm with the axially varying radius given by

$$\frac{r(x)}{r_0} = 1 + 0.3 \sin\left(\frac{\pi x}{L}\right) + 0.4 \sin\left(\frac{2\pi x}{L}\right) + 0.2 \cos\left(\frac{3\pi x}{L}\right), \quad (11)$$

where $r_0 = 100 \mu\text{m}$. The meniscus position $\ell(t)$ was obtained for imbibition in both directions by numerically integrating Eqs. (2) and (3) using the Runge–Kutta method, with $\alpha = 0.18$ m. To mimic experimental noise in the measured data, Gaussian random noise with a zero mean and standard deviation of $10 \mu\text{m}$ was added to the numerically obtained values of $\ell(t)$; this was considered as the measured data. Thereafter, the measured data were filtered using a 3-point moving average filter, and the meniscus speeds $u_f(x)$ and $u_r(x)$ were obtained by numerically differentiating the smoothed $\ell(t)$ vs t curves. These meniscus speeds were subsequently used to compute $f(x)$ and then $r(x)$ using Eq. (10). Figure 2(a) shows that the

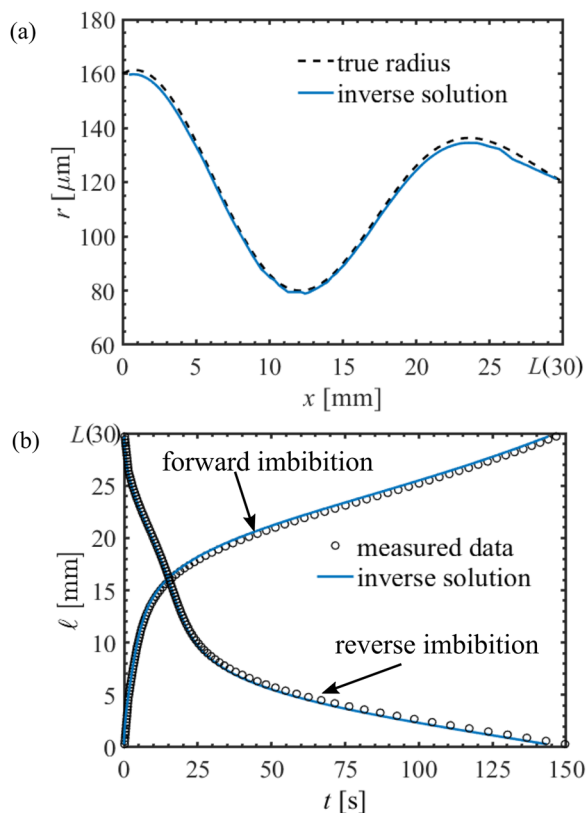


FIG. 2. Validation of the analytical solution for the inverse problem of capillary imbibition using simulated imbibition kinematics. (a) Comparison of the capillary radius determined by solving the inverse problem with the true capillary radius given by Eq. (11). The capillary radius predicted using the analytical solution compares well with the true radius. (b) Comparison of the measured imbibition kinematics with those obtained by solving the forward imbibition problem using the predicted capillary radius. The imbibition kinematics corresponding to the predicted capillary radius agree well with the measured data. In these calculations, random noise was added to the simulated data of imbibition length $\ell(t)$ vs t , to mimic experimental uncertainty, and the resulting data were considered as the measured data.

radius estimated by solving the inverse problem using Eq. (10) is in excellent agreement with the true capillary radius given by Eq. (11). Moreover, as shown in Fig. 2(b), the meniscus position $\ell(t)$ predicted by solving the forward problem using the estimated radius matches well with the measured ℓ vs t data. Note that the small deviations in the predicted and true radii and the corresponding imbibition kinematics are due to the random noise added to the imbibition data. In the absence of any added noise, the predicted radius matches exactly with the true radius of the capillary.

Next, we demonstrate the applicability of our approach for determining the capillary radius from experimentally measured imbibition data. To this end, we consider the experiments of Elizalde *et al.*,¹³ wherein a glass capillary with a non-uniform cross section was fabricated by heating and pulling the capillary. A mixture of glycerol and 2-propanol with $\alpha = 0.18$ m was used for the imbibition experiments. The meniscus position during the imbibition in forward and reverse directions was recorded using a CCD camera. For our analysis, we digitized the experimental data of

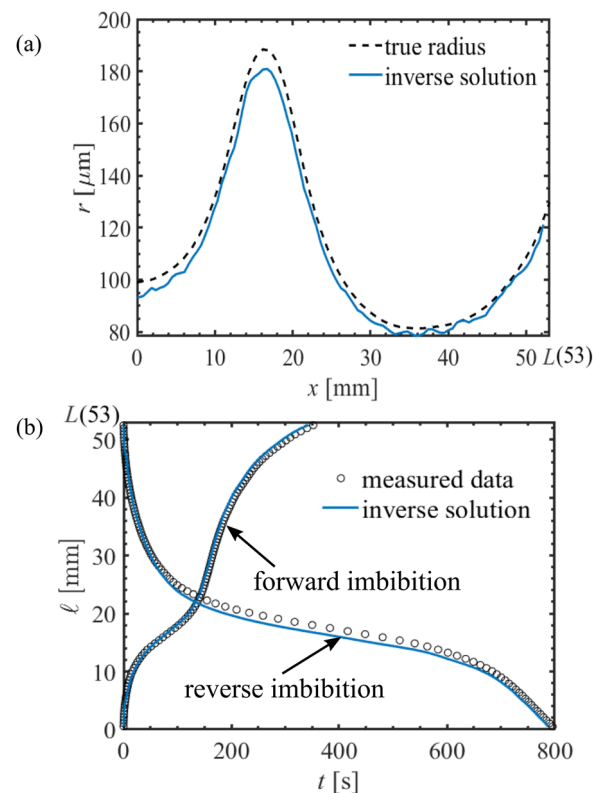


FIG. 3. Validation of the analytical solution for the inverse problem of capillary imbibition using experimental data of Elizalde *et al.*¹³ (a) Comparison of the capillary radius determined by solving the inverse problem with the experimentally determined true capillary radius. The capillary radius predicted using the analytical solution compares well with the true radius. (b) Comparison of the time-varying imbibition length, $\ell(t)$ vs t , measured during experiments with those obtained by solving the forward imbibition problem using the predicted capillary radius. The imbibition kinematics corresponding to the predicted capillary radius agree well with the experimental data.

imbibition kinematics and the actual radius of the capillary, reported by Elizalde *et al.*¹³ Following a similar procedure to that described for the first problem, we used the experimental data to obtain the capillary radius $r(x)$, using Eq. (10). Figure 3(a) shows a comparison of the radius $r(x)$ predicted by Eq. (10) with the actual radius of the capillary measured using the camera. Despite the uncertainty in digitized experimental data, the solution to the inverse problem agrees well with the actual radius of the capillary. Figure 3(b) shows the variation of the meniscus position with time measured during the forward and reverse imbibition experiments. The imbibition kinematics simulated using the radius curve obtained by solving the inverse problem are also in agreement with the experimental data, as shown in Fig. 3(b). These results demonstrate the robustness of the analytical solution to measurement uncertainties.

To summarize, we have presented a closed-form analytical solution of the inverse problem of capillary imbibition, which involves determination of the radius of an axially non-uniform capillary using experimentally measured data of imbibition kinematics. Unlike the previous iterative methods proposed to solve this inverse problem, our method gives a direct solution. We have validated our method with data of capillary imbibition obtained from numerical simulations and experimental measurements of capillary imbibition. The analytical solution of the inverse capillary imbibition problem can be helpful in determining the internal geometry of micro- and nano-porous structures in a non-destructive manner and design of autonomous capillary pumps for microfluidic applications.

We acknowledge the financial support received from the Science and Engineering Research Board (SERB), Government of India, under the Impacting Research Innovation and Technology (IMPRINT-2) scheme (Grant No. IMP/2018/000422).

The data that support the findings of this study are available within the article.

REFERENCES

- ¹P. Zhang, M. T. Tweheyo, and T. Austad, "Wettability alteration and improved oil recovery by spontaneous imbibition of seawater into chalk: Impact of the potential determining ions Ca^{2+} , Mg^{2+} , and SO_4^{2-} ," *Colloids Surf., A* **301**, 199–208 (2007).
- ²F. Schwillie, "Groundwater pollution in porous media by fluids immiscible with water," in *Studies in Environmental Science* (Elsevier, 1981), Vol. 17, pp. 451–463.
- ³M. Dejam, H. Hassanzadeh, and Z. Chen, "Reinfiltration through liquid bridges formed between two matrix blocks in fractured rocks," *J. Hydrol.* **519**, 3520–3530 (2014).
- ⁴S. Ashraf, G. Visavale, S. S. Bahga, and J. Phirani, "Spontaneous imbibition in parallel layers of packed beads," *Eur. Phys. J. E* **40**, 39 (2017).
- ⁵N.-T. Nguyen, S. A. M. Shaegh, N. Kashaninejad, and D.-T. Phan, "Design, fabrication and characterization of drug delivery systems based on lab-on-a-chip technology," *Adv. Drug Delivery Rev.* **65**, 1403–1419 (2013).
- ⁶L. Gervais and E. Delamarche, "Toward one-step point-of-care immunodiagnostics using capillary-driven microfluidics and PDMS substrates," *Lab Chip* **9**, 3330–3337 (2009).
- ⁷J. M. Bell and F. K. Cameron, "The Flow of Liquids through Capillary Spaces," *J. Phys. Chem.* **10**, 658–674 (1906).
- ⁸R. Lucas, "Ueber das zeitgesetz des kapillaren Aufstiegs von Flüssigkeiten," *Kolloid Z.* **23**, 15–22 (1918).
- ⁹E. W. Washburn, "The dynamics of capillary flow," *Phys. Rev.* **17**, 273 (1921).
- ¹⁰M. Reyssat, L. Courbin, E. Reyssat, and H. A. Stone, "Imbibition in geometries with axial variations," *J. Fluid Mech.* **615**, 335–344 (2008).
- ¹¹A. Budaraju, J. Phirani, S. Kondaraju, and S. S. Bahga, "Capillary displacement of viscous liquids in geometries with axial variations," *Langmuir* **32**, 10513–10521 (2016).
- ¹²M. Hultmark, J. M. Aristoff, and H. A. Stone, "The influence of the gas phase on liquid imbibition in capillary tubes," *J. Fluid Mech.* **678**, 600–606 (2011).
- ¹³E. Elizalde, R. Urteaga, R. R. Koropecski, and C. L. Berli, "Inverse problem of capillary filling," *Phys. Rev. Lett.* **112**, 134502 (2014).
- ¹⁴E. Elizalde, R. Urteaga, and C. L. A. Berli, "Rational design of capillary-driven flows for paper-based microfluidics," *Lab Chip* **15**, 2173–2180 (2015).
- ¹⁵M. Zimmermann, H. Schmid, P. Hunziker, and E. Delamarche, "Capillary pumps for autonomous capillary systems," *Lab Chip* **7**, 119–125 (2007).